Supplemental Figures

Figure S1

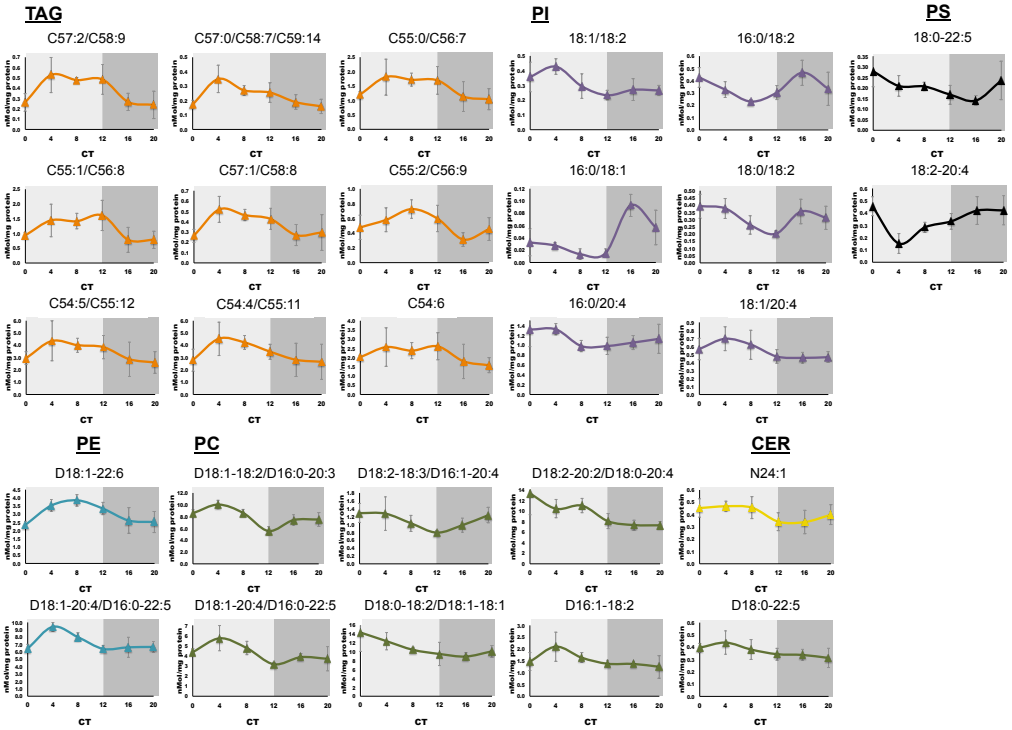

Figure S2

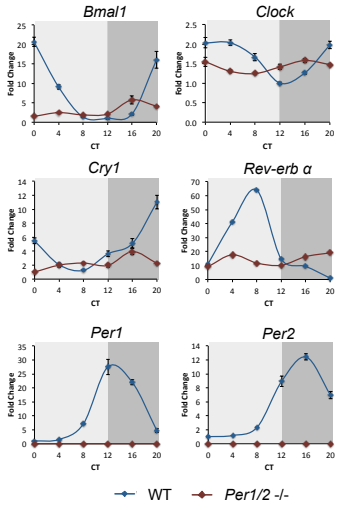

Figure S3

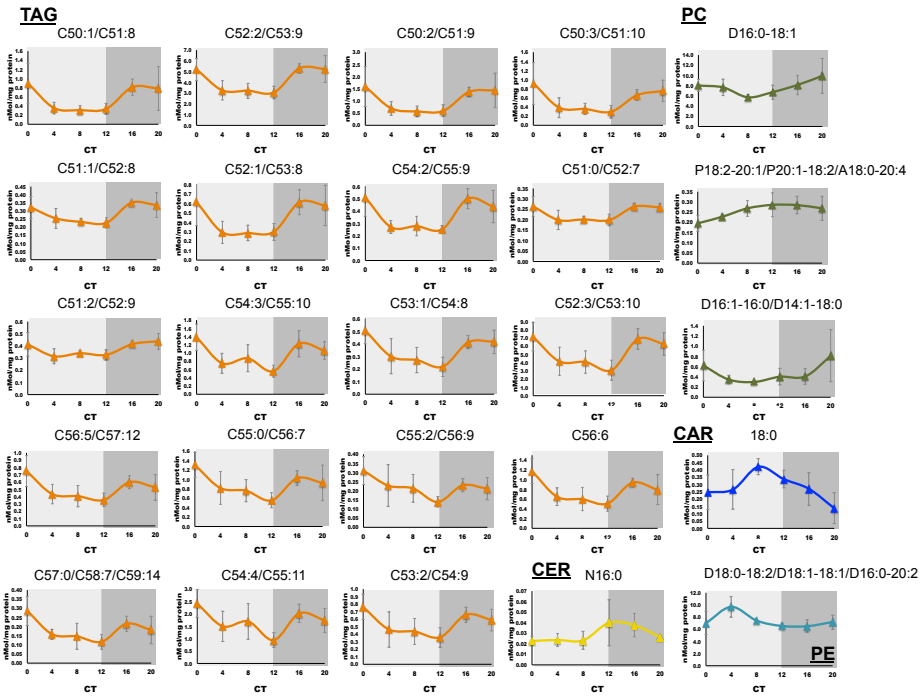

Figure S4

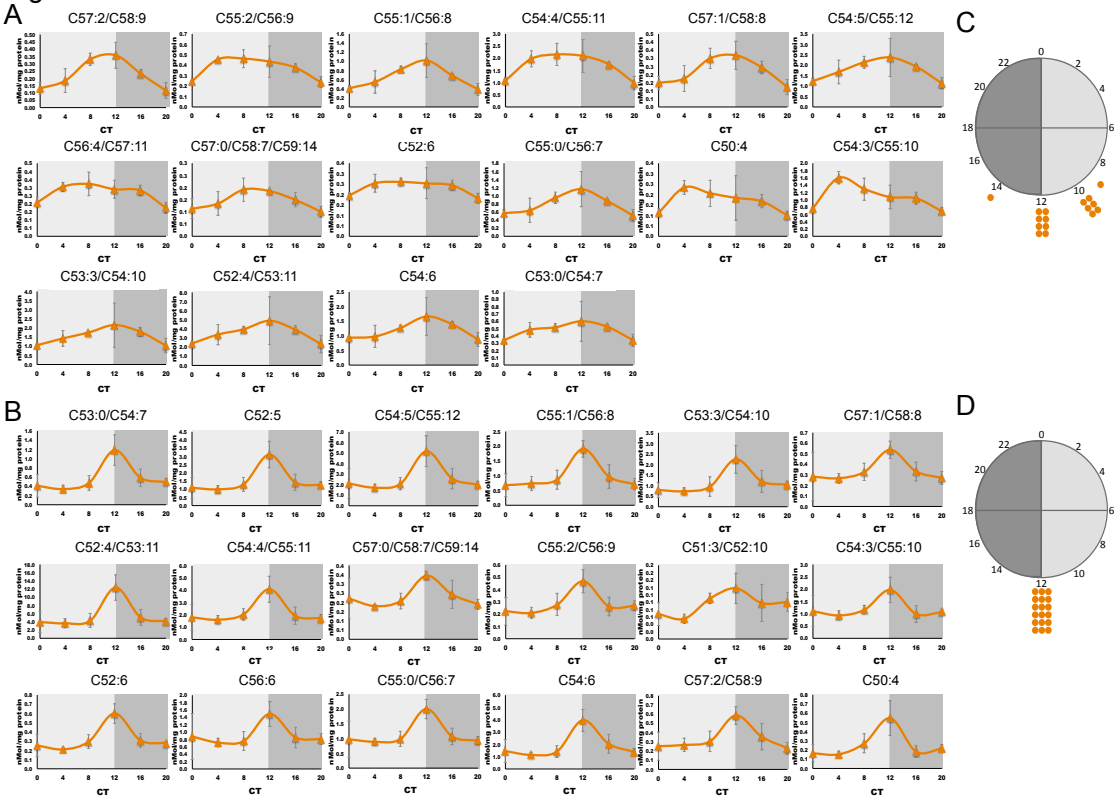

Figure S5

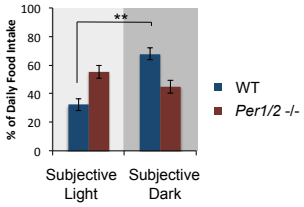

Figure S6

A

TAG species:

C50:4
C51:3/C52:10
C52:4/C53:11
C52:5
C52:6
C53:0/C54:7
C53:3/C54:10
C54:3/C55:10
C54:4/C55:11
C54:5/C55:12
C54:6
C55:0/C56:7
C55:1/C56:8
C55:2/C56:9
C56:4/C57:11
C56:6
C57:0/C58:7/C59:14
C57:1/C58:8
C57:2/C58:9

B

TAG species:

C50:1/C51:8
C50:2/C51:9
C50:3/C51:10
C51:0/C52:7
C51:1/C52:8
C51:2/C52:9
C52:1/C53:8
C52:2/C53:9
C52:3/C53:10
C53:1/C54:8
C53:2/C54:9
C54:2/C55:9
C56:5/C57:12

C

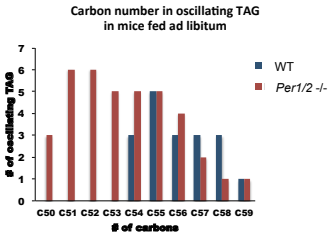

D

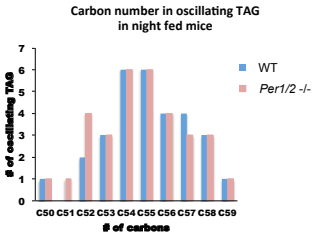

Figure S7

A

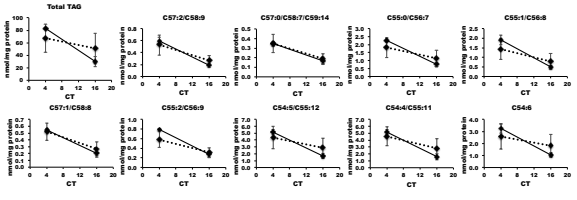

B

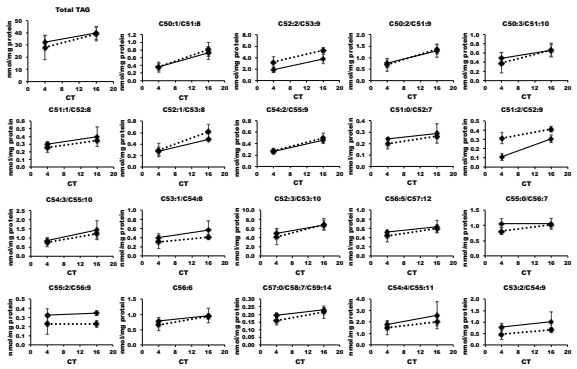

C

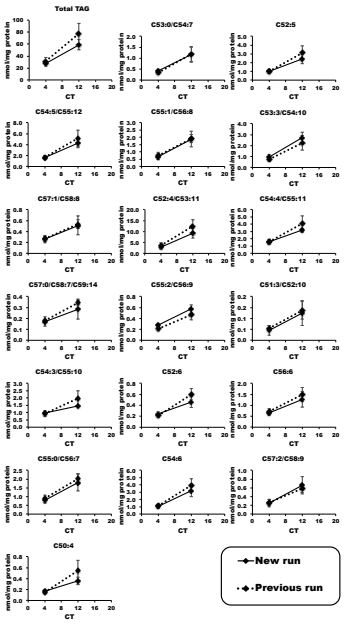

Supplemental Figure Legends

Figure S1, related to Figure 1. Accumulation profiles of oscillating lipids in WT mice fed ad libitum. WT mice were fed ad libitum and sacrificed under constant darkness, at 4 h intervals throughout the day. Livers were harvested and lipids were analyzed and quantified by shotgun lipidomics. Oscillating lipids were determined based on JTK_CYCLE analysis (6 time points, n=4 for each, *P* value <0.05). Data are presented as mean +/- STDEV. Circadian Time (CT).

Figure S2, related to Figure 3. Circadian expression profiles of core clock genes. WT and *Per1/2* null mice were sacrificed under constant darkness, at 4 h intervals throughout the day. Total RNA was prepared from liver and mRNA expression levels of *Bmal1*, *Clock*, *Cry1, Rev-erba, Per1, and Per2* were measured by quantitative real-time PCR and presented as fold change relative to the lowest value. Data are presented as mean +/- STDEV, with a mix of 4 animals per time point. Circadian Time (CT).

Figure S3, related to Figure 3. Accumulation profiles of oscillating lipids in *Per1/2* null mice fed ad libitum. *Per1/2* null mice were fed ad libitum and sacrificed under constant darkness, at 4 h intervals throughout the day. Livers were harvested and lipids were analyzed and quantified by shotgun lipidomics. Oscillating lipids were determined based on JTK_CYCLE analysis (6 time points, n=4 for each, *P* value <0.05). Data are presented as mean +/- STDEV. Circadian Time (CT).

Figure S4, related to Figure 4. Accumulation profiles of oscillating TAG in WT and *Per1/2* null mice fed exclusively during the night. WT mice and *Per1/2* null mice were fed exclusively during the night and sacrificed at 4 h intervals throughout the day. Livers were harvested and TAG were analyzed and quantified by shotgun lipidomics. Oscillating TAG

were determined based on JTK_CYCLE analysis (6 time points, n=3 for WT mice and n=4 for *Per1/2* null mice per each time point, *P* value <0.05). Accumulation profiles of oscillating TAG in WT mice **(A)** and *Per 1/2* null mice **(B)** fed exclusively during the night. Day-time distribution of peak phases of oscillating TAG in WT mice **(C)** and *Per 1/2* null mice **(D)**. Data are presented as mean +/- STDEV. Circadian Time (CT).

Figure S5, related to Figure 4. Daily distribution of food intake in WT and *Per1/2* null mice. The amount of food consumed throughout the day was measured using metabolic cages in WT and *Per1/2* null mice fed ad libitum. Mice were maintained under a 12 h light/dark regimen for several consecutive days, during the last day of the experiment the light was turned off and measurements were performed under constant darkness. The data are presented on a bar graph (mean +/- SEM, 8 mice for each genotype) as percentage of the amount of food consumed in each phase (i.e. subjective light, subjective dark) relatively to the total food consumption during the day. Dark gray represents the subjective night and light gray the subjective day. *P* value < 0.01 is marked in **.

Figure S6, related to Figure 5. Dissection of oscillating TAG species. A., List of oscillating TAG species that appear to respond to feeding fasting cycles (i.e. all identified oscillating TAG except for the one that exclusively oscillated in *Per1/2* -/- mice fed ad libitum). **B.,** List of oscillating TAG species that exclusively oscillated in *Per1/2* -/- mice fed ad libitum. **C., and D.,** Oscillating TAG species were plotted based on their carbon number. In case a single TAG species shared more than one annotation, all designated annotations were plotted. **C.,** Comparison of WT and *Per1/2* -/- mice fed ad libitum. **D.,** Comparison of WT and *Per1/2* -/- mice fed exclusively during the night.

Figure S7, related to Figure 4. Two time point analysis of TAG measurements in WT mice fed ad libitum and *Per1/2 -/-* mice fed either ad libitum or night fed. TAG species were quantified (3 additional mice per time point) for two time points that corresponds to the nadir and zenith levels of TAG accumulation in WT mice fed ad libitum and *Per1/2 -/-* mice fed either ad libitum or night fed. The data were plotted and compared with the original dataset presented in Figures S1, S3 and S4B. **A.,** WT mice fed ad libitum. **B.,** *Per1/2 -/-* mice fed ad libitum. **C.,** *Per1/2 -/-* mice night fed. Continues line represents the new run, dashed line represents the previous run. Data are presented as mean +/- STDEV (n=3 for the new run and n=4 for the previous run). See also Table S6.

Supplemental Table Legends

Table S1 related to Figure 1. Analysis of lipids measured and quantified in WT mice fed ad libitum. Excel sheet A., WT mice were fed ad libitum and sacrificed under constant darkness, at 4 h intervals throughout the day. Livers were harvested and lipids were analyzed and quantified by shotgun lipidomics. Absolute levels are presented in nmol/mg protein, 4 individual mice per time point. **Excel sheet B.,** The nonparametric JTK_CYCLE algorithm was used to identify lipids that display diurnal rhythmicity in WT mice fed ad libitum. Lipids are ordered based on their *P* value. Lipids that were considered as false positives are marked in red. ADJ.P: Permutation based *P* value, LAG: Optimal phase, AMP: Amplitude, PER: Period.

Table S2 related to Figure 3. Analysis of lipids measured and quantified in *Per1/2* -/- mice fed ad libitum. Excel sheet A., *Per1/2* -/- mice were fed ad libitum and sacrificed under constant darkness, at 4 h intervals throughout the day. Livers were harvested and lipids were analyzed and quantified by shotgun lipidomics. Absolute levels are presented in nmol/mg protein, 4 individual mice per time point. **Excel sheet B.,** The nonparametric JTK_CYCLE algorithm was used to identify lipids that display diurnal rhythmicity in *Per1/2* -/- mice fed ad

libitum. Lipids are ordered based on their *P* value. Lipids that were considered as false positives are marked in red. ADJ.P: Permutation based *P* value, LAG: Optimal phase, AMP: Amplitude, PER: Period.

Table S3 related to Figure 4. Analysis of TAG measured and quantified in WT mice fed exclusively during the dark phase. Excel sheet A., WT mice were fed exclusively during the dark phase and sacrificed at 4 h intervals throughout the day. Livers were harvested and TAG were analyzed and quantified by shotgun lipidomics. Absolute levels are presented in nmol/mg protein, 3 individual mice per time point. **Excel sheet B.,** The nonparametric JTK_CYCLE algorithm was used to identify TAG that display diurnal rhythmicity in WT mice fed exclusively during the dark phase. TAG are ordered based on their *P* value. ADJ.P: Permutation based *P* value, LAG: Optimal phase, AMP: Amplitude, PER: Period.

Table S4 related to Figure 4. Analysis of TAG measured and quantified in *Per1/2* -/- mice fed exclusively during the dark phase. Excel sheet A., *Per1/2* -/- mice were fed exclusively during the dark phase and sacrificed at 4 h intervals throughout the day. Livers were harvested and TAG were analyzed and quantified by shotgun lipidomics. Absolute levels are presented in nmol/mg protein, 3 individual mice per time point. **Excel sheet B.,** The nonparametric JTK_CYCLE algorithm was used to identify TAG that display diurnal rhythmicity in *Per1/2* -/- mice fed exclusively during the dark phase. TAG are ordered based on their *P* value. ADJ.P: Permutation based *P* value, LAG: Optimal phase, AMP: Amplitude, PER: Period.

Table S5 related to Figure 6. Total TAG levels quantified throughout the day for each TAG species. Total TAG levels were quantified throughout the day in WT fed ad libitum, WT night fed, *Per1/2* -/- fed ad libitum and *Per1/2* -/- night fed mice. Each set is the sum of 6

individual mice covering all 6 CTs. There are for 4 different sets for WT fed ad libitum, *Per1/2* -/- fed ad libitum and *Per1/2* -/- night fed mice and 3 different sets for WT night fed mice.

Table S6 related to Figure 4. Two time point analysis of TAG measurements in WT mice fed ad libitum and *Per1/2 -/-* mice fed either ad libitum or night fed. TAG species were quantified (3 additional mice per time point) for two time points that correspond to the nadir and zenith levels of TAG accumulation for each one of the experimental setup. **Excel sheet A.,** CT4 and CT16 for WT mice fed ad libitum. **Excel sheet B.,** CT4 and CT16 for *Per1/2 -/-* mice fed ad libitum. **Excel sheet C.,** CT4 and CT12 for *Per1/2 -/-* mice night fed. Data are presented in absolute values for each sample with the corresponding t-test value for each species comparing previous and new runs for each CT. T-test with values <0.05 are marked in red. Oscillating TAG species are marked in blue.

Supplemental Experimental Procedures

Shotgun lipidomic analysis

The methodology employed in this manuscript can detect and quantify numerous TAG species in mouse liver. Obviously, we cannot exclude the fact that some TAG species are not detected; however we have good reasons to believe that this fraction is negligible. In principle, the undetected TAG fraction could come from two major sources. Either due to incomplete recovery of TAG species from the extraction, or due to missed detection by the 2D-MS method. However, since we spike an internal standard into each sample prior to the lipid extraction and the analysis is conducted relative to the internal standard, the incomplete recovery estimated in our method is very low. For the detection of some fatty acids by the 2D-MS method, we omitted the detection of odd carbon-numbered fatty acids out in the current study due to resource consideration. This fraction of fatty acids in mouse liver TAG pool only counts for less than 3%. Accordingly, we believe that the detected fraction of TAG species is

higher than 95% (Han et al., 2008; Yang et al., 2009). However, since the vast majority of them is in minute amounts, we included in our analysis only the most abundant TAG species (35 species) that represent ~95% of the total TAG mass in the liver. This hepatic TAG pool primarily serves as an energy depot, and is affected by food intake, activity levels and lipid metabolism.

Chemical used:

Methyl-tert-butyl ether (Fisher Scientific, Fair Lawn, NJ)

Methanol (Burdick and Jackson, Muskegon, MI)

Millipore deionized water

Isopropanol (Burdick and Jackson, Muskegon, MI)

Lithium hydroxide (Sigma-Aldrich, St. Louis, MO)

Lipid Internal Standards used:

All of the lipid internal standards are purchased from Avanti Polar Lipids, Inc., Alabaster, AL, except the noted ones.

1,2-Dimyristoleoyl-sn-glycero-3-phosphocholine (di14:1 PC)

1,2-Dipalmitoleoyl-sn-glycero-3-phosphoethanolamine (di16:1 PE)

1,2-Dipentadecanoyl-sn-glycero-3-phosphoglycerol (sodium salt) (di15:0 PG)

1,2-Dimyristoyl-*sn*-glycero-3-phospho-L-serine (sodium salt) (di14:0 PS)

1,2-Dimyristoyl-*sn*-glycero-3-phosphate (sodium salt) (di14:0 PA)

1,1',2,2'-Tetramyristoyl cardiolipin (T14:0 CL)

N-Lauroryl sphingomyelin (N12:0 SM)

N-Heptadecanoyl ceramide (N17:0 Cer)

1-Heptadecanoyl-2-hydroxy-*sn*-glycero-3-phosphocholine (17:0 lysoPC)

1,2,3,4-13C4-Palmitoyl-L-carnitine hydrochloride ($^{13}C_4$-16:0 CAR) (Sigma-Aldrich, St. Louis, MO)

Triheptadecenoin (T17:1 TAG) (Nu Chek, Inc. Elysian, MN)

A list of primers and probes used for quantitative real-time PCR.

For quantitative real-time PCR both TaqMan probes and SYBR green assay were employed.

Gene Name	Primer/Probe sequences
Tbp	Forward primer 5'-CCCTATCACTCCTGCCACACCAGC-3' Reverse primer 5'-GTGCAATGGTCTTTAGGTCAAGTTTACAGCC-3'
Hprt	Forward primer 5'-GGCCAGACTTTGTTGGATTTG-3' Reverse primer 5'-TGCGCTCATCTTAGGCTTTGT-3'
Gapdh	Forward primer 5'-AGGTCGGTGTGAACGGATTTG-3' Reverse primer 5'-TGTAGACCATGTAGTTGAGGTCA-3'
Gpat1	Forward primer 5'-ACAGTTGGCACAATAGACGTTT-3' Reverse primer 5'-CCTTCCATTTCAGTGTTGCAGA-3'
Gpat2	Forward primer 5'-TGAACCGCCTCTTCCTGAATG-3' Reverse primer 5'-CGGGAGTCTAAAGCCACACG-3'
Agpat1	Forward primer 5'-TAAGATGGCCTTCTACAACGGC-3' Reverse primer 5'-CCATACAGGTATTTGACGTGGAG-3'
Agpat2	Forward primer 5'-CTTCAAGTACGTGTATGGCCTT-3' Reverse primer 5'-CTGTGAACATTAGCTCACGCT-3'
Lpin1	Forward primer 5'-CTCCGCTCCCGAGAGAAAG-3' Reverse primer 5'-TCATGTGCAAATCCACGGACT-3'
Lpin2	Forward primer 5'-GAAGTGGCGGCTCTCTATTTC-3' Reverse primer 5'-AGAGGGTTACATCAGGCAAGT-3'
Dgat1	Forward primer 5'-CTGATCCTGAGTAATGCAAGGTT-3' Reverse primer 5'-TGGATGCAATAATCACGCATGG-3'
Dgat2	Forward primer 5'-GCGCTACTTCCGAGACTACTT-3' Reverse primer 5'-GGGCCTTATGCCAGGAAACT-3'
Lipa	Forward primer 5'-TGCCCACGGGAACTGTATC-3' Reverse primer 5'-ATCCCCAGCGCATGATTATCT-3'
Pnpla3	Forward primer 5'-TCCAACTTCTGACCAGAGCG-3' Reverse primer 5'-ACAGATGCCATTCTCCTCCAG-3'
PPAR alpha	Forward primer 5'-AACATCGAGTGTCGAATATGTGG-3' Reverse primer 5'-CCGAATAGTTCGCCGAAAGAA-3'
PPAR gamma	Forward primer 5'-CTCCAAGAATACCAAAGTGCGA-3' Reverse primer 5'-GCCTGATGCTTTATCCCCACA-3'
SREBP1c	Forward primer 5'-GGAGCCATGGATTGCACATT-3' Reverse primer 5'-GGCCCGGGAAGTCACTGT-3'
Per1	Forward primer 5'-ACCAGCCATTCCGCCTAAC-3' Reverse primer 5'-CGGGGAGCTTCATAACCAGA-3'
Per2	Forward Primer 5'-ATGCTCGCCATCCACAAGA-3' Reverse Primer 5'-GCGGAATCGAATGGGAGAAT-3' Probe 5'-FAM-ATCCTACAGGCCGGTGGACAGCC-TAMRA-3'
Bmal1	Forward Primer 5'-CCAAGAAAGTATGGACACAGACAAA-3' Reverse Primer 5'-GCATTCTTGATCCTTCCTTGGT-3' Probe 5'-FAM-TGACCCTCATGGAAGGTTAGAATATGCAGAA-TAMRA-3'
Rev-erb a	Forward Primer 5'-TGCAGGCTGATTCTTCACACA-3' Reverse Primer 5'-AGCCCTCCAGAAGGGTAGGA-3' Probe 5'-FAM-ACACTCTCTGCTCTTCCCATGCAAATCAG-TAMRA-3'

Cry1	Forward Primer 5'-CTGGCGTGGAAGTCATCGT-3' Reverse Primer 5'-CTGTCCGCCATTGAGTTCTATG-3' Probe 5'-FAM-CGCATTTCACATACACTGTATGACCTGGACA-TAMRA-3'
Clock	Forward Primer 5'- AGAACTTGGCATTGAAGAGTCTC-3' Reverse Primer 5'- GTCAGACCCAGAATCTTGGCT-3'

Supplemental References

Han, X., Yang, K., and Gross, R.W. (2008). Microfluidics-based electrospray ionization enhances the intrasource separation of lipid classes and extends identification of individual molecular species through multi-dimensional mass spectrometry: development of an automated high-throughput platform for shotgun lipidomics. Rapid Commun Mass Spectrom 22, 2115-2124.

Yang, K., Cheng, H., Gross, R.W., and Han, X. (2009). Automated lipid identification and quantification by multidimensional mass spectrometry-based shotgun lipidomics. Anal Chem 81, 4356-4368.